Fragmentation of a liquid metal jet into water

Nicolas Rimbert*[1], Hadj-Achour Miloud[1], Gradeck Michel[1], Labergue Alexandre[1], and Renaud Meignen[2]

[1]Laboratoire des Energies et de la Mécanique Théorique et Appliquée : UMR7563 Université de Lorraine-Centre National de la Recherche Scientifique (Université de Lorraine - ENSEM, 2 avenue de la Forêt de Haye, TSA 60604, 54518 Vandœuvre-lès-Nancy Cedex, France)

[2]Service des Accidents Graves, Institut de Radioprotection et de Sûreté Nucléaire (Cadarache, Saint Paul Lez Durance 13115, France)

*Corresponding author: nicolas.rimbert@univ-lorraine.fr

Abstract

This paper presents experimental results on the fragmentation of a low meting point liquid metallic alloy jet into water. The liquid is Field's metal whose melting point is 62 °C. Data are obtained using high-speed camera acquisition and the solidified particles are sieved, a size Probability Distribution Function (PDF) is obtained from their mass distribution. These results are compared to separate data acquisitions obtained using a phase Doppler anemometer (PDA used in reflexion regime). Injection diameter range from 1 mm to 5 mm and injection velocity from 2.28 m/s to 4.97 m/s resulting in a Weber number ranging from 26 to 309 and a Reynolds number ranging from 4577 to 24875. The conclusion is that for these intermediate Weber and Reynolds numbers, the size of the droplets can mainly be related to Kelvin-Helmholtz instabilities. However, there exists also a long tail of small sized droplet whose distribution can be attributed to turbulent re-agglomeration of ligaments. This part of the distribution is very close to a log-Lévy law thanks to a model developed by [Rimbert & Castanet, PhysRevE, 84, 016318, 2011] By estimating the different turbulent scales, it is even possible to construct the small size distribution of droplet without using any fitting parameter.

Keywords

Jet Fragmentation Instabilities Turbulence Lévy Stable Law

Introduction

Atomization and Sprays have a wide range of applications. The present paper is dedicated to the study of liquid-liquid fragmentation with high density ratio. Its main application is the understanding of severe nuclear accident where molten corium can interact with surrounding water. The residual heat of 3000°C hot Corium makes this interaction mostly water vapour/corium; nevertheless, the use of low(er)-melting point alloy is a classical way of recovering both the high-density density ratio and the high surface tension of the melt while working in simpler and safer conditions [1,2]. The present study goes one step further in the simplification as overheating of the molten metal is such that no vapour is ever produced. This allows for the use of optical methods (shadowgraphy, Phase Doppler Anemometer…etc.). The strategy is to use these more precise measurements to build more precise models that could eventually be used on the real case.

As far as atomization modelling is concerned, recent advances on the modelling of this topic, mostly concerns the influence of ligament intermediate in the fragmentation process [3], though not really new (see [4] for instance), the main idea here is that it leads to a Gamma distribution of the daughter droplets. However, no leads to how-to compute parameters of the Gamma distribution has been found in the general case up to now. This seems to compete with Kolmogorov analysis [5] leading to log-normal distribution which has been recently modernized [6]. In this case also, the computation of the parameters un the general case is difficult though some models do exist. Last, competition between classical instabilities such as Rayleigh-Taylor instability or Kelvin-Helmholtz instabilities is known to be fundamental, at least near the instability threshold. This led to quite intricate models such as [7] which are still used nowadays in commercial Computer Fluid Dynamics codes. [8] presents a synthesis of these three kinds of modelling based on the following assumptions: (i) instabilities do govern the triggering of the fragmentation process and the size of the largest fragments; (ii) formation of the final droplet is mediated by transitory ligament-shaped blobs of liquids; (iii) final size of the droplet is governed by interaction of the ligaments with surrounding turbulence. This results in a fine-size droplet PDF that can be approximated by a log-stable law. These laws are generalisations of log-normal laws and are sometimes known as universal multifractals [9,10]. [11] gives an explanation (self-avoiding vortex tangles) for their importance in the modelling of fine-scale structure of turbulence but most importantly also gives a way to compute every parameters of the distribution. This allows [8]

This work is licensed under a Creative Commons 4.0 International License (CC BY-NC-ND 4.0).

to propose a model to compute the fine-size droplet PDF in a fan-spray. The purpose of present work is to show how this work allows for the computation of the fine-size droplet PDF in the present liquid-liquid case.

Material and methods

The experimental set-up is a modification of the set-up used in [12] himself derived from a drop-on-demand device as conceived in [13]. The liquid metal injector is represented on figure 1. It uses Field's metal a eutectic alloy of Tin, Bismuth and Indium whose melting temperature is 62°C. The temperature of the melt (85°C) is maintained by a "bain-marie" technique. The measured density of Field's metal 7994 kg/m^3, its viscosity is approximately 10 mPa.s (and very sensitive to oxidation when tested in a Couette viscosimeter) and its surface tension is 0.41 N/m when compared to water (it has been measured by the ADSA technique).

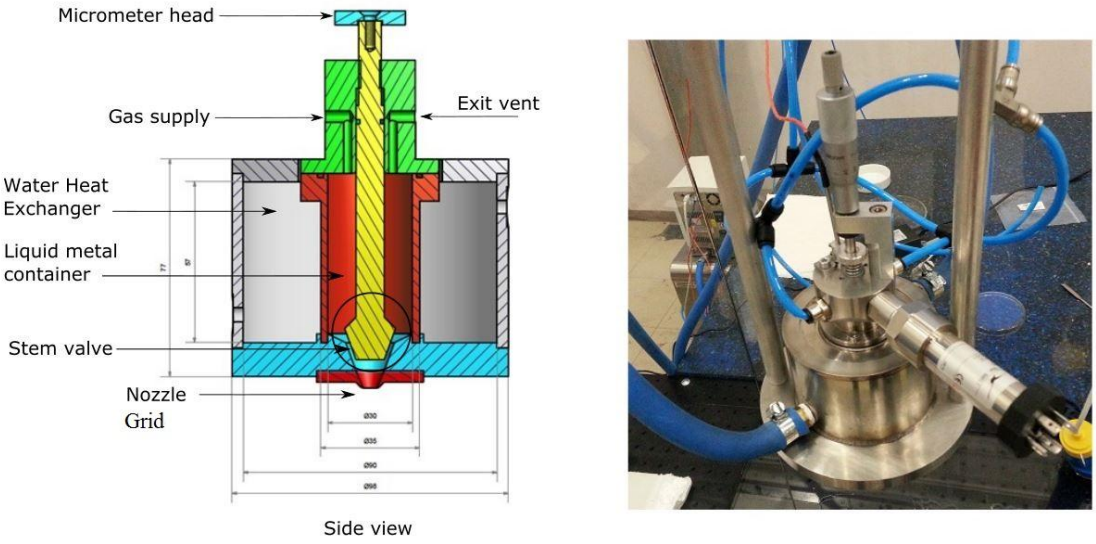

Figure 1. GaLad experimental Set-up. This is based on a drop-on-demand technique such as developed in [13].

The GaLaD experimental setup has been modified to include an electro-magnet that allows for the opening of the stem-valve for a longer time thereby generating a jet (henceforth named JaLaD). The velocity of the jet is controlled by varying the pressure of the Nitrogen gas-supply. The new set-up as well as the set-up of the Dantec Phase Doppler Anemometer is shown on figure 2. The size of the water pool is 50cmx50cmx40cm and is heated to 40°C. The jet disintegrates in the water but the droplets solidify before they hit the bottom of the vessel and are eventually collected to be sieved.

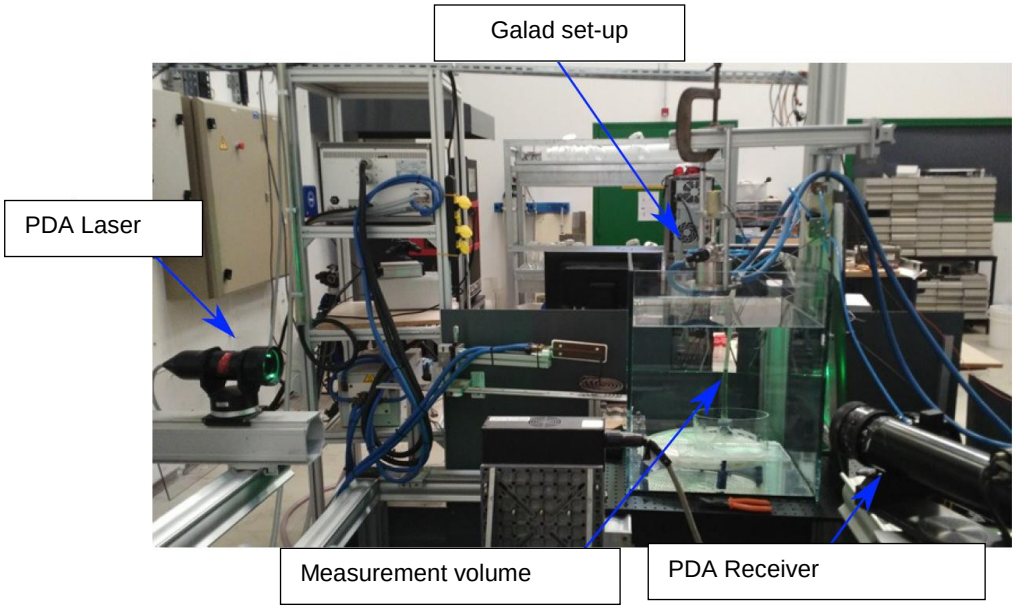

Figure 2. JaLaD experimental set-up for liquid metal jet into water. The Dantec PDA system is set in reflexion mode.

This work is licensed under a Creative Commons 4.0 International License (CC BY-NC-ND 4.0).

As mentioned three measurement techniques are used to study the jet disintegration. The first technique is high speed shadowgraphy. Imaging is obtained thanks to a LED lighting (PRIOLITE LED 400 equivalent to 400W halogen light) and a phantom V701 high speed camera. The second is a Dantec PDA system whose configuration is given on table 1 (it allows measurement two velocity components and the size of the droplets). The third system is the simpler: it consists in a Retsch vibratory sieve shaker AS 200 which is used to separate the fragments according to their size. Each bin is thereafter weighted.

Table 1. Configuration of the Dantec PDA system

Parameter	Value
Green laser wavelength	514.5 (nm)
Blue laser wavelength	488 (nm)
Laser Beam Waist Radii	1.35 (mm)
Distance between separated laser beams	60 (mm)
Emission focal length	1200 (mm)
Reception focal length	500 (mm)
PDA scaling factor	1
Observation angle	80°
Measurement angle (between beams)	0.05°
Green measurement volume	23.3mmx0.58mm
Blue measurement volume	22.1mmx0.55mm

Results and discussion

The four non dimensional parameters governing the hydrodynamics of the fragmentation are:

$$We = \frac{\rho_C U_0^2 D_0}{\gamma} \tag{1}$$

$$Oh = \frac{\mu_L}{\sqrt{D_0 \rho_L \gamma}} \tag{2}$$

$$\rho_R = \frac{\rho_L}{\rho_C} \tag{3}$$

$$\mu_R = \frac{\mu_L}{\mu_C} \tag{4}$$

where ρ is the density, μ is the dynamic viscosity, γ is the surface tension, D_0 is the jet nozzle diameter and U_0 the jet initial velocity, subscript C indicate the property of the carrier phase while subscript L indicate the property of the liquid (metal) phase. In the present case, the Weber number is the main hydrodynamic parameter.

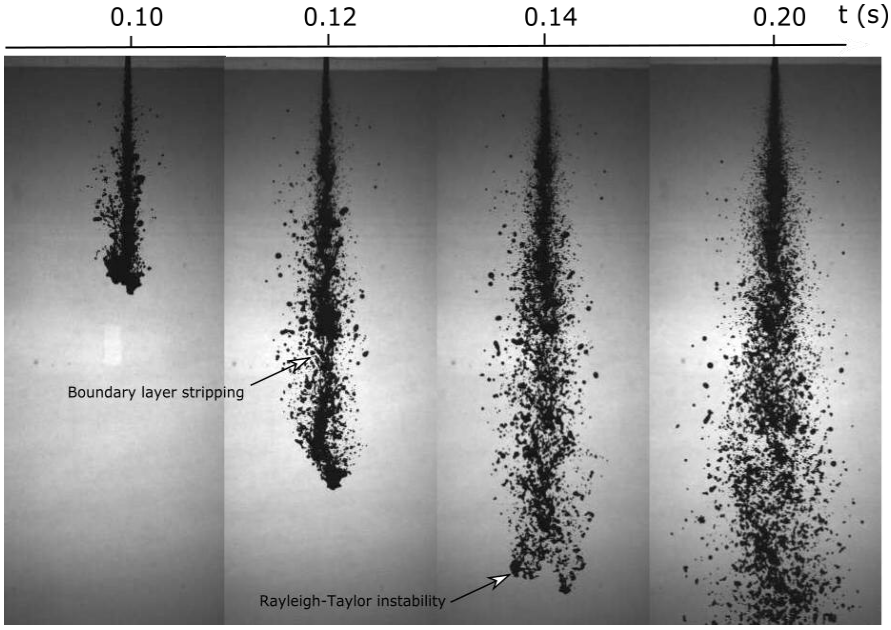

Figure 3. Shadowgraph images for D2P6 experiment.

This work is licensed under a Creative Commons 4.0 International License (CC BY-NC-ND 4.0).

Figure 3 shows a sample shadowgraph. The measure of the tip penetration speed gives us an estimate of the jet velocity U_0. Table 2 indicate the four different experimental conditions for the combined shadowgraph/sieving experiments. Table 3 indicate the resulting of the sieving of the solidified fragments in for four separate case (summarized by their Weber number). The values of Sauter Mean Diameter and Mass Mean Diameter (MMD) given in table (2) are computed from table (3) using equations (5) and (6).

Table 2. Experimental conditions for the high-speed shadowgraphy and the sieving experiments.

Test n°	D_0	Pressure	U (m/s)	We	SMD/D_0	MMD/D_0
D2P6	2 mm	6 bar	2.3	26.45	0.147	0.32
D2P10	2 mm	10 bar	2.8	39.2	0.098	0.21
D5P6	5 mm	6 bar	4.3	200	0.056	0.15
D5P10	5 mm	10 bar	4.8	288	0.040	0.12

Table 3. Sieving of the solidified fragments bold. Experimental condition are given on table 3

	20 µm	50 µm	100 µm	500 µm	1000 µm	2000 µm	Total Mass
We = 288	1.1 g	2.4 g	19.2 g	33.0 g	57.3 g	11.6 g	124.6 g
We = 200	0.4 g	1.7 g	15.5 g	23.2 g	60.7 g	30.6 g	132.1 g
We = 39.2	0.6 g	1.2 g	24.7 g	59.2 g	23.9 g	45.8 g	132.9 g
We = 26.45	0.3 g	0.9 g	10.9 g	34.7 g	60.7 g	13.4 g	120.4 g

$$MMD = \sum_{i=0}^{N_s} x_i \bar{D}_i \tag{5}$$

$$SMD = \frac{1}{\sum_{i=0}^{N_s} x_i / \bar{D}_i} \tag{6}$$

where $\bar{D}_i = (D_i + D_{i+1})/2$ is the "average" bin sieve diameter. The corresponding Mass PDF are represented on figure 4. For comparison the following characteristic length scale are computed: the wavelengths associated to the Kelvin-Helmhotlz (eq. 7) and Rayleigh-Taylor instabilities (eq. 8). Hinze characteristic size of maximum stable globules in turbulence [14] is given by equation (9).

$$\lambda_{KH} = \frac{3\pi\gamma(\rho_C + \rho_L)}{U_0^2 \rho_C \rho_L} \tag{7}$$

$$\lambda_{RT} = 2\pi\sqrt{\frac{3\gamma}{g(\rho_L - \rho_C)}} \tag{8}$$

where *g* is gravity acceleration.

$$D_{Hinze} = \left(\frac{2\gamma}{\rho_L}\right)\left(\frac{5}{2}\right)^{2/5} \varepsilon^{-2/5} \tag{9}$$

Note that to compute Hinze's diameter, the average turbulent kinetic energy dissipation rate ε is needed. It is estimated as usual through equation (10).

$$\varepsilon \cong \frac{u'^3}{L_{\text{int}}} \tag{10}$$

Where u' represents the fluctuating velocity around the statistical average (Reynolds decomposition). Note that this allows for the computation of Taylor's characteristic turbulent length scale and Kolmogorov's length scale through equation (11) and (12).

$$\lambda = \sqrt{20\nu\frac{k}{\varepsilon}} \tag{11}$$

$$\eta \cong \left(\frac{\nu^3}{\varepsilon}\right)^{1/4} \tag{12}$$

In either eq. (10) or eq. (11), the kinetic energy of turbulence *k* is computed assuming that u'~U which is usually true for turbulent jets. Table 4 summarizes the results of such order of magnitude computations. It can be seen that Rayleigh Taylor instability wavelength is not of the good magnitude and is therefore ruled out as a possible

This work is licensed under a Creative Commons 4.0 International License (CC BY-NC-ND 4.0).

mechanism for fragmentation. Likewise, it can be seen that the order of magnitude of the small droplet seems to be close to the Taylor length-scale suggesting that the smallest droplet must be influenced by the turbulence generated in the fluid.

Table 4. Experimental conditions for the high-speed shadowgraphy and the sieving experiments.

Test n°	We	U (m/s)	λ_{RT}/D_0	λ_{KH}/D_0	ε (m^2/s^3)	λ/D_0	η/D_0	D_{Hinze}/D_0
D2P6	26.45	2.3	13.13	0.400	6083.5	0.0351	$1.8\ 10^{-3}$	0.0880
D2P10	39.2	2.8	13.13	0.270	10976	0.0261	$1.5\ 10^{-3}$	0.0695
D5P6	200	4.3	5.26	0.046	39753	0.0055	$4.48\ 10^{-4}$	0.0166
D5P10	288	4.8	5.26	0.037	55296	0.0047	$4.12\ 10^{-4}$	0.0146

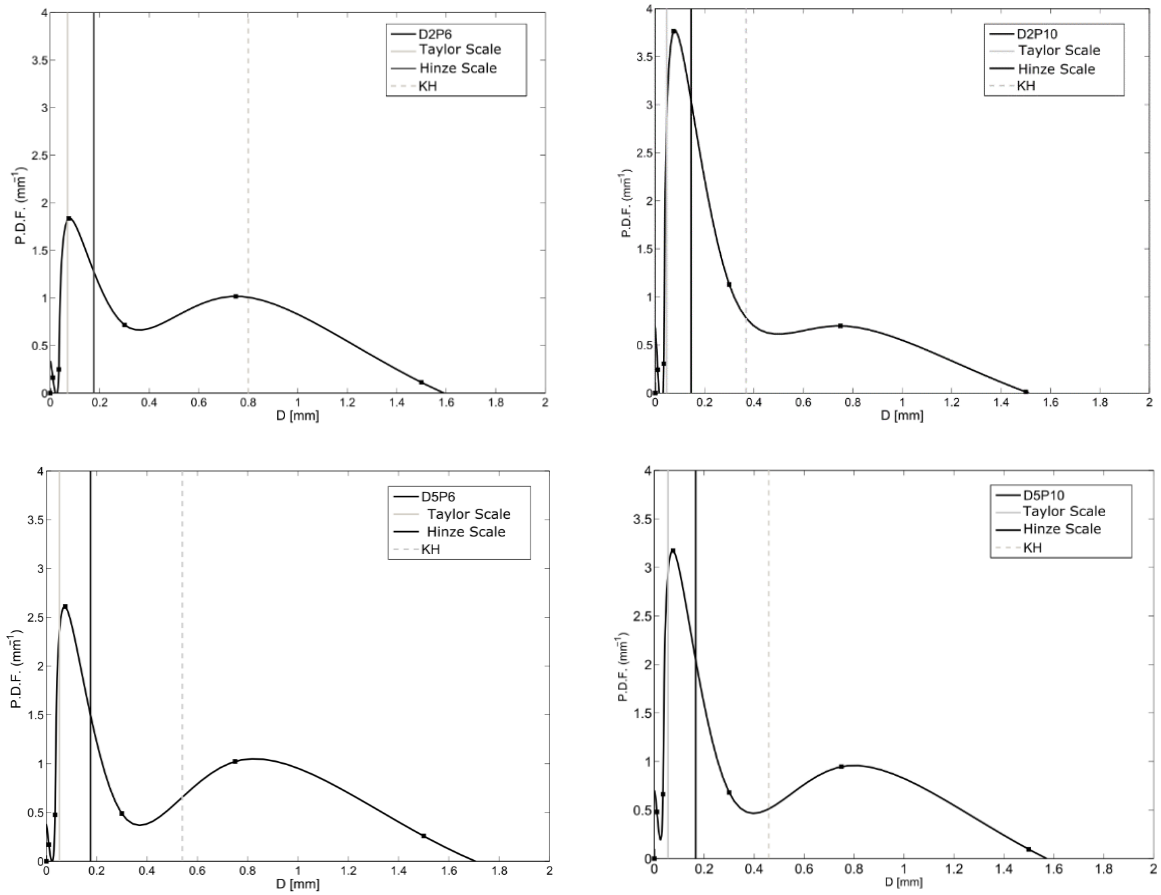

Figure 4. Comparison of the Mass PDF obtained from the sieving technique for the four considered cases.

These considerations are confirmed more rigorously thanks to the PDA measurements. Unfortunately, it was not possible to use the 2mm and 5mm nozzle in the PDA case. As JaLaD experiment is a converted drop-on-demand apparatus, it can only contain roughly 120g of liquid metal. Therefore, it empties quite quickly and a 1 mm nozzle was needed for this special case to make the jet last longer. Note that this creates a systematic error on the diameter obtained by sieving, as the last droplets produced can be gas-blown by a sudden release of gas when the injection ends and the container is empty thus generating smaller droplets. Also related to small size of the container, the calibration of the PDA was mainly done using glass beads in order to simplify the process. Injection pressure was 6 bar. The results in an injection velocity close to 2.5 m/s and a jet Weber number close to 15. Figure 5 shows the joint size-velocity PDF that has been measured out of 10,000 droplets (it was not possible to get greater sample again due to the limited size of the container). The measurement point is located 10cm below the nozzle and 1cm off axis. It can therefore be supposed that all the atomization process has stopped when the droplets are caught in the measurement volume. It is interesting to see that all the droplets seem to have the same velocity (close to 1m/s) when this happens. It can also be seen that the fluctuations around this average velocity are great and can be evaluated to be also of the order of 1 m/s therefore generating 100% turbulence intensity, which is usual in turbulent jets.

This work is licensed under a Creative Commons 4.0 International License (CC BY-NC-ND 4.0).

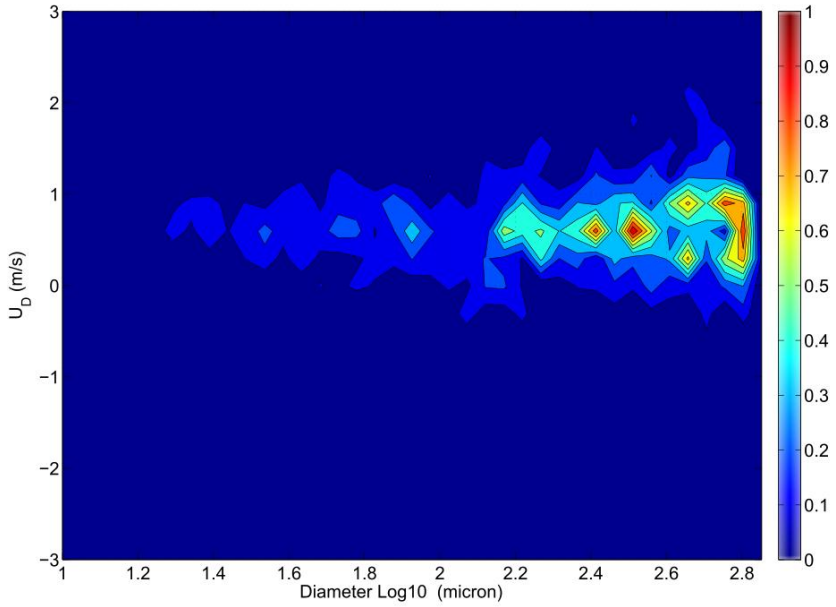

Figure 5. Size-Velocity measurements obtained from the PDA analysis. Measurement point is located 10 cm below the injector, 1cm slightly off axis.

As their velocity seems to be constant, it is therefore possible to compute the size PDF of the droplet independently from their velocity. This is what is done on figure 6. Note that the cut-off of the PDA related to the shape of the measurement volume (env. 565µm if taking the average of the two bands cf. table 1) can be evaluated to be $\log_{10}$ (565) = 2.75 while the measurements can be estimated to be precise until 316 µm ($\log_{10}$(316) = 2.5). Note that the Kelvin-Helmholtz wavelength is not in the measurement range as:

$$\lambda_{KH} = 3\pi \frac{0.41(1000+7994)}{2.5^2 \times 1000 \times 7994} \approx 695\mu m \tag{13}$$

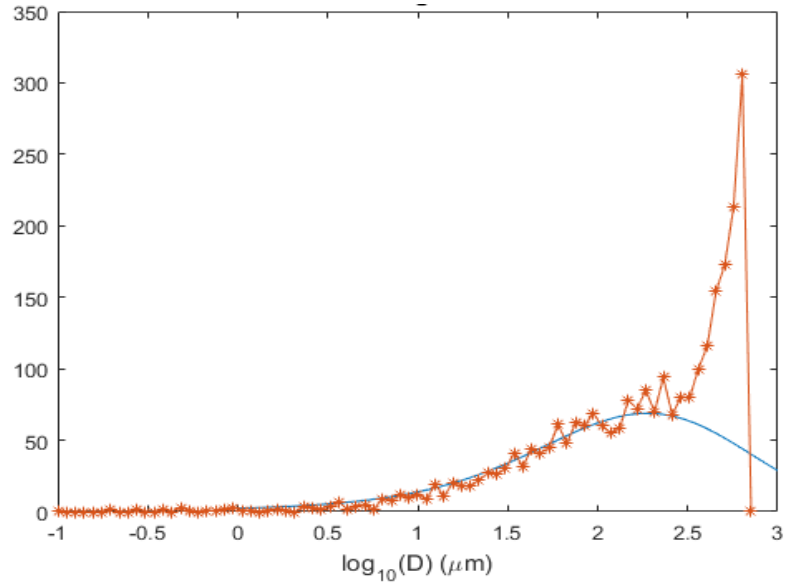

Figure 6. Number of droplets collected by the PDA according to the logarithm of their size.

Figure 6 also shows as a blue line, the results of the log-stable model developed in [8]. Let us recall how Lévy stable laws are defined [15]:

"A random variable X is said to have a stable distribution denoted $p_\alpha(x;\beta,\sigma,\delta)$ if there are real parameters $0<\alpha\leq 2$, $0<\sigma$, $-1\leq\beta\leq 1$ and δ such that its characteristic function has the following form:

$$\hat{p}_\alpha(k;\beta,\sigma,\delta) = \exp\left(ik\delta - \sigma^\alpha |k|^\alpha \left[1 + i(sign(k))\beta\omega(|k|,\alpha)\right]\right) \tag{14}$$

This work is licensed under a Creative Commons 4.0 International License (CC BY-NC-ND 4.0).

where $\omega(|k|,\alpha)=\begin{cases}\tan(\alpha\pi/2) & \text{if } \alpha\neq 1\\ -(2/\pi)\log|k| & \text{if } \alpha=1\end{cases}$ (15) "

Simply put, the four parameters are respectively, α, the stability index governing the tail of the distribution, β the skewness parameter governing the symmetry of the law, δ the shift parameter governing the position of the maximum of the distribution and σ the scale parameter governing the width of the distribution. Gaussian laws are special cases of Lévy laws with parameter α = 2, β indifferent, δ being the average and σ the standard deviation. Except in the Gaussian case, Lévy laws are not square integrable, the standard deviation cannot usually be defined, hence the name scale parameter. Note that present modeling generalizes log-normal laws and not Gaussian laws as it is applied to the distribution of the logarithm of the diameter. [11] shows that the value that should be used to describe turbulence intermittency are α = 1.7, β = -1 (note that the distribution are said totally skewed to the left and that the resulting log-stable distribution has finite moments of all positive orders). Moreover σ can be computed using equation (16)

$$\sigma_{\ln\varepsilon}^{\alpha}=\ln\frac{\lambda}{\eta}=3,43 \tag{16}$$

Where Taylor and Kolmogorov scales defined in eq. (11) and (12) are estimated using eq. (17) therefore leading to values given by eq. (18) and (19).

$$\varepsilon\cong\frac{u'^3}{L_{\text{int}}}\cong\frac{1^3}{1.10^{-3}}\cong 1000\ m^2/s^3 \tag{17}$$

$$\lambda=\sqrt{20\nu\frac{1,5}{1000}}\ ;\ 173\mu m\ \left(\text{Log}_{10}(173)=2,23\right) \tag{18}$$

$$\eta\cong\left(\frac{\nu^3}{\varepsilon}\right)^{1/4}\cong 5,6\mu m \tag{19}$$

The droplet size PDF is related to the preceding PDF through the relation given by eq. (20) and (21). Details of the model can be found in [8] but let us recall that the physical idea is that the ligaments produced during the fragmentation process are re-agglomerated due to the surrounding turbulence (interaction between ligaments and surrounding vortices).

$$\delta_{\ln d}=Log_{10}(\lambda)=2.23 \tag{20}$$

$$\sigma_{\ln d}=\frac{1}{2}\sigma_{\ln\varepsilon}=\frac{1}{2}(3,43)^{\frac{1}{1.7}}\approx 1.0 \tag{21}$$

Figure 6 shows the result of the superposition of Lévy stable laws with parameters α = 1.7, β = -1, $\delta = \delta_{\text{lnd}}$, $\sigma = \sigma_{\text{lnd}}$. No fitting is made and only the vertical axis (i.e. the number of droplets obeying to the proposed law) is varied. The result is therefore quite encouraging.

Conclusions

Results for the fragmentation statistics of a jet of liquid Field's metal in hot water are provided. Analysis shows that Kelvin-Helmholtz instability can be related to the greatest mass of the daughter droplet. However, there exists a tail of small daughter droplets that extend to the size of the smallest vortices produced by the turbulence generated by the jet. The scenario proposed in [8] concerning the turbulent re-agglomeration process of the ligaments produced during the primary fragmentation of the jet seems to be able to reproduce the small size PDF without any need for adjustment. However, the amount of mass going into each channel (Kelvin-Helmholtz or turbulence) remains to be determined. This will be possible by increasing the jet Weber number which would however a new experimental facility.

Acknowledgements

The work was done under the research program on nuclear safety and radioprotection (RSNR) and received funding from French government managed by the National Research Agency (ANR) under Future Investments Program (PIA), research grant No: ANR-10-RSNR-01.

This work is licensed under a Creative Commons 4.0 International License (CC BY-NC-ND 4.0).

References

[1] Pilch, M. et Erdman, C. (1987). Use of breakup time data and velocity history data to predict the maximum size of stable fragments for acceleration-induced breakup of a liquid drop. International Journal of Multiphase Flow, 13(6):741–757.
[2] Gelfand, B. (1996). Droplet breakup phenomena in flows with velocity lag. Progress in Energy and Combustion Science, 22(3):201–265.
[3] Villermaux, E., Marmottant, P., & Duplat, J. (2004). Ligament-mediated spray formation. *Physical review letters*, *92*(7), 074501.
[4] Dombrowski, N., & Johns, W. R. (1963). The aerodynamic instability and disintegration of viscous liquid sheets. *Chemical Engineering Science*, *18*(3), 203-214.
[5] Kolmogorov, A. N. (1941). On the lognormal distribution law of the dimensions of particles under pulverization. In Doklady of the Akademy of Sciences of the USSR, volume 31, pages 99–101.
[6] Gorokhovski, M. A. et Saveliev, V. L. (2003). Analyses of Kolmogorov's model of breakup and its application into Lagrangian computation of liquid sprays under air-blast atomization. Physics of Fluids, 15(1):184–192.
[7] Beale, J. C., & Reitz, R. D. (1999). Modeling spray atomization with the Kelvin-Helmholtz/Rayleigh-Taylor hybrid model. *Atomization and sprays*, *9*(6).
[8] Rimbert, N., & Castanet, G. (2011). Crossover between Rayleigh-Taylor instability and turbulent cascading atomization mechanism in the bag-breakup regime. *Physical Review E*, *84*(1), 016318.
[9] Mandelbrot, B. B. (1982). *The fractal geometry of nature*. New York: WH freeman.
[10] Schertzer, D., & Lovejoy, S. (1987). Physical modeling and analysis of rain and clouds by anisotropic scaling multiplicative processes. *Journal of Geophysical Research: Atmospheres*, *92*(D8), 9693-9714
[11] Rimbert, N. (2010). Simple model for turbulence intermittencies based on self-avoiding random vortex stretching. *Physical Review E*, *81*(5), 056315.
[12] Hadj-Achour M., Rimbert N., Meignen R., Gradeck M. Study of Secondary Fragmentation of Liquid Metal Droplets in a Water Pool in revision for International Journal of Multiphase Flow
[13] Amirzadeh, A., Raessi, M. et Chandra, S. (2013). Producing molten metal droplets smaller than the nozzle diameter using a pneumatic drop-on-demand generator. Experimental Thermal and Fluid Science, 47:26–33.
[14] Hinze, J. O. (1949). Critical speeds and sizes of liquid globules. Flow, Turbulence and Combustion, 1(1), 273.
[15] Samorodnitsky, G., & Taqqu, M. (1994). Non-Gaussian Stable Processes: Stochastic Models with Infinite Variance. *Chapman ft Hall, London*.

This work is licensed under a Creative Commons 4.0 International License (CC BY-NC-ND 4.0).